aerospace

MDPI

Article

Test Results for a Novel 20 kW Two-Phase Pumped Cooling System for Aerospace Applications

Henk Jan van Gerner [1,*], Tim Luten [1], Sigurd Scholten [1], Georg Mühlthaler [2] and Marcus-Benedict Buntz [3]

[1] NLR-Royal Netherlands Aerospace Centre, 1059 CM Amsterdam, The Netherlands; tim.luten@nlr.nl (T.L.); sigurd.scholten@nlr.nl (S.S.)
[2] Airbus Commercial Aircraft, 22335 Hamburg, Germany; georg.muehlthaler@airbus.com
[3] Aerostack GmbH, 72581 Dettingen, Germany; marcus-benedict.buntz@airbus.com
* Correspondence: henk.jan.van.gerner@nlr.nl

Abstract: In the EU-funded BRAVA project, technologies for a fuel cell-based power generation system for aviation are being developed. In this paper, the test results for a demonstrator of a novel two-phase pumped cooling system with 20 kW cooling capacity are presented. This system uses the evaporation of a liquid to remove waste heat from the heat sources. Several concepts have been tested with this demonstrator, including the 'no accumulator' concept, which offers a large mass reduction compared to conventional cooling systems. Additionally, the system can be rotated, and the influence of the orientation has been tested.

Keywords: two-phase; cooling; pump; methanol; fuel cell; accumulator

1. Introduction

1.1. Background

Hydrogen energy holds significant potential in the clean energy transition for transportation, industry, and construction [1]. Proton Exchange Membrane (PEM) fuel cells transform the chemical energy liberated during the electrochemical reaction of hydrogen and oxygen into electrical energy [2]. Fuel cells (FC) can operate at a higher efficiency than hydrogen gas combustion turbine engines, and because of the relatively low operating temperature (<120 °C) compared to hydrogen combustion engines, they exhaust only water and no NO_x emissions. Hydrogen-powered PEM fuel cells are therefore the preferred energy source for electric aircraft [3]. For this reason, technologies for an FC-based power generation system for aircraft capable of carrying up to 100 passengers on distances of up to 1000 nautical miles are being developed in the EU-funded BRAVA (Breakthrough Fuel Cell Technologies for Aviation) project [4]. One of these technologies is the cooling system for the FC. An FC system generates a significant amount of waste heat that has to be removed with a cooling system, and this cooling system represents a significant part of the total system mass. For the application of FC in aircraft, it is of utmost importance to reduce the mass of the cooling system. Large FC systems in vehicles are typically cooled with liquid Ethylene Glycol–Water (EGW) mixtures. In [5], a comparison was made with numerical simulations of a conventional liquid EGW cooling system and two-phase cooling systems. The comparison showed that the mass of a liquid EGW system is 35% higher than that of two-phase cooling with an accumulator and using methanol as a coolant. Furthermore, the mass of a liquid EGW system is 2.4 times higher than that of a two-phase cooling system when a novel 'no accumulator' concept is used. In order to investigate the feasibility and

check for updates

Academic Editor: Andreas Strohmayer, Spiros Pantelakis and Nikolaos Michailidis

Received: 3 December 2024
Revised: 13 February 2025
Accepted: 18 February 2025
Published: 26 February 2025

Citation: van Gerner, H.J.; Luten, T.; Scholten, S.; Mühlthaler, G.; Buntz, M.-B. Test Results for a Novel 20 kW Two-Phase Pumped Cooling System for Aerospace Applications. *Aerospace* **2025**, *12*, 188. https://doi.org/10.3390/aerospace12030188

behaviour of a two-phase cooling (2-PC) system with methanol, a test setup with 20 kW cooling capacity was built. The test results of this setup are described in this paper.

1.2. What Is a Two-Phase Pumped Cooling System?

Two-phase cooling systems were originally developed for space applications, for example, for the thermal control system of the Alpha Magnetic Spectrometer (AMS-02), which is mounted on the International Space Station [6]. Additionally, commercial spacecraft from Thales Alenia Space have 2-PC systems [7], and 2-PC systems are being developed for active antennae for communication satellites [8]. More recently, 2-PC systems are being developed for the cooling of power electronics modules for electric aircraft motors [9,10]. Figure 1 shows a schematic drawing of a 2-PC system. A pump transports liquid to an evaporator, which consists of cooling plates that are integrated into the fuel cell stack. In the evaporator, the waste heat from the fuel cells is absorbed, and the liquid (partially) turns into vapor (i.e., the term 'two-phase' refers to the phase transition of the fluid from liquid to vapor). The vapor/liquid mixture then flows to the condenser. In the condenser, the absorbed heat from the FC is transferred to the air that flows through the ram air heat exchanger, and the vapor is turned back into liquid. The saturation temperature in the system depends on the pressure, and this pressure is controlled by the accumulator [8–10]. The accumulator also allows for fluid density changes (e.g., as a result of evaporation) in the loop.

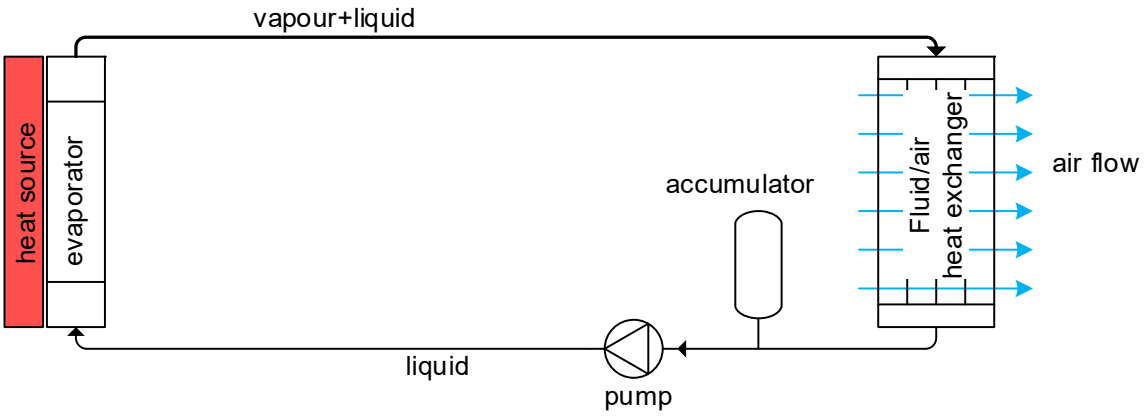

Figure 1. Schematic drawing of a 2-PC system.

The schematic of a 2-PC system is very similar to that of a liquid EGW cooling system that is commonly used for fuel cells, except that in a 2-PC system, the liquid is evaporated. This results in several advantages:

- The required mass flow is an order of magnitude smaller. This results in significantly lower electrical power consumption by the pump and a much smaller pump mass. Additionally, the piping diameter can be smaller, which reduces the overall mass of the system.
- Freezing of the fluid under low ambient temperatures (−55 °C) is not possible, since the freezing point of methanol is −97 °C.
- Due to the low freezing point and high heat transfer coefficient of two-phase methanol, it is easier to use the waste heat from the fuel cell to warm liquid H_2 before it enters the fuel cell.
- The heat transfer coefficient for evaporating or condensing flow is typically much higher than the heat transfer coefficient for liquid flow. This results in a smaller temperature difference between the fluid and the heat exchanger walls.

A disadvantage compared to liquid cooling is that the accumulator of a 2-PC system has to be considerably larger. Furthermore, the design is more complex.

2. Description of the Setup

Figure 2 shows a schematic drawing of the 20 kW two-phase cooling (2-PC) system, Figures 3–5 show CAD drawings, and Figure 6 shows photos. The system has 16 parallel evaporator plates divided into two parallel branches. The heat load of 20 kW is generated by foil heaters attached to the evaporator plates. The system has four fluid-air heat exchangers that function as condensers (see Figure 5). For the methanol flow, the condensers are in a parallel configuration. A fan is used to force air from inside the system through the condensers to the outlet air duct. For the airflow, the condensers are placed in two parallel branches, with two condensers in series in each branch. The airflow through the condensers can be (partially) blocked by inserting a plate between the air duct and the condenser (see Figure 5). The system has two flowmeters. The difference between the measured flow of these flowmeters can be used to determine the methanol flow into and out of the accumulator. The saturation temperature in the system depends on the pressure, and this pressure is controlled by the accumulator. Most 2-PC systems have a Heat-Controlled Accumulator (HCA) [6–10]. In an HCA, both vapor and liquid are present, and the saturation temperature in the system is controlled by a heater on the vessel. The main advantage of an HCA is that it is relatively simple. Disadvantages of an HCA are the energy consumption of the heater, and the sensitivity to the direction of acceleration. Instead of an HCA, it is also possible to use a Pressure-Controlled Accumulator (PCA). To the authors' knowledge, there are no descriptions of systems with a PCA available in the literature. In a PCA, only subcooled liquid and no vapor is present and the pressure of the liquid in the accumulator can be controlled with pressurized air or N_2 gas which is separated from the liquid by a bellows, bladder, or diaphragm. The 20 kW system uses a PCA, which consists of a 5 L expansion vessel with an EPDM bladder. The setup has four viewing glasses with cameras to monitor the flow pattern and the presence of gas bubbles at several locations. The system also has a motorized control valve to bypass the condenser. With this setup, the following have been tested:

- Saturation temperature control using a PCA.
- Influence of orientation by rotating the system.
- Different methods for controlling the evaporator inlet temperature.
- Influence of blocked airflow through a condenser.
- Testing of the 'no accumulator' concept. For this, the system is equipped with a valve between the accumulator and the loop.
- Testing of the 'small accumulator' concept. For this, the 5 L vessel is replaced with a 1 L vessel.

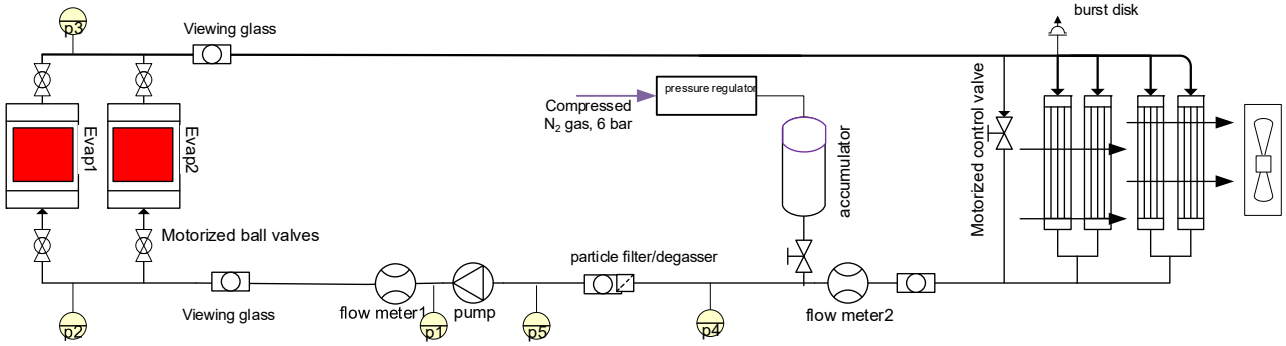

Figure 2. Schematic drawing of the 20 kW test setup.

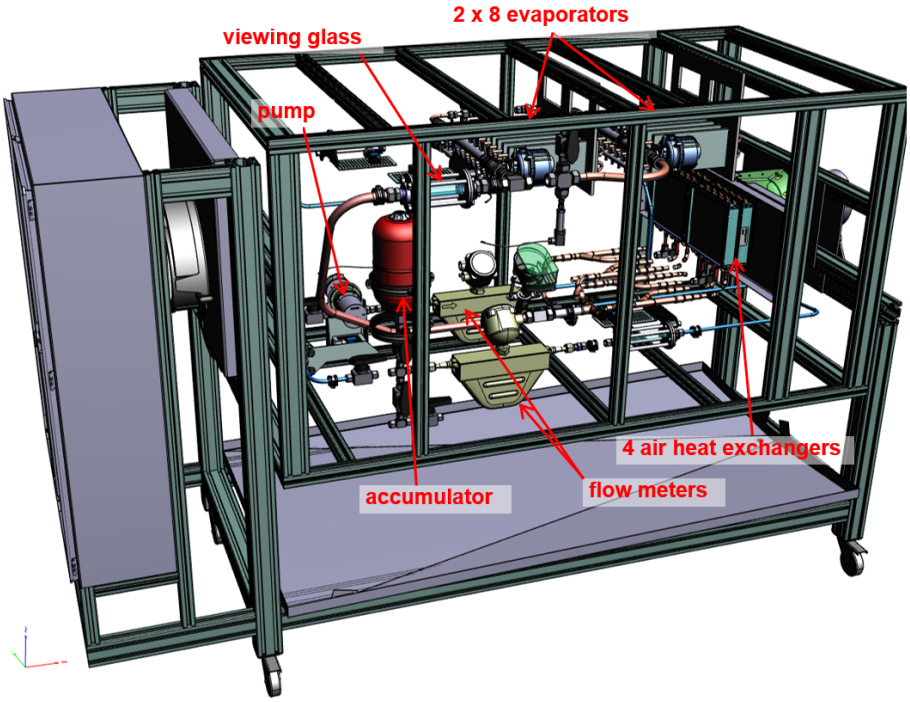

Figure 3. CAD drawing of the 20 kW test setup.

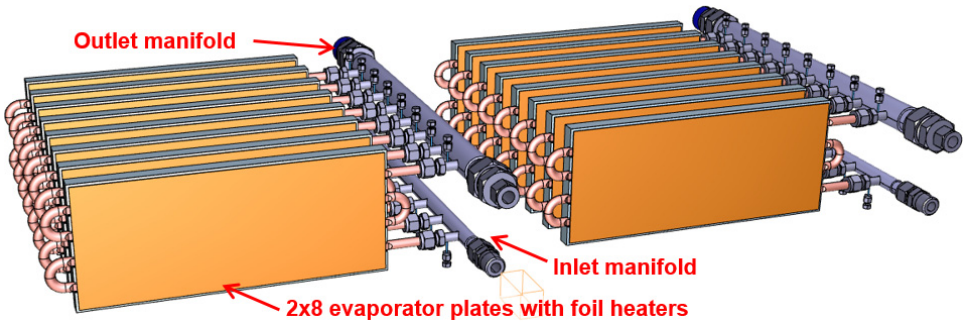

Figure 4. CAD drawing of the evaporator section.

The main components of the system and the measurement accuracies of the sensors are included in Table 1.

Table 1. Main components of the system, including the accuracies of sensors.

Description	Manufacturer	Type	Accuracy
Pump	Gather (Wülfrath, Germany)	Series 2, 30/10	
Flowmeters (2×)	Emerson (Rijswijk, The Netherlands)	Micro Motion R050S Coriolis Meter	0.75% (0.5 g/s at 60 g/s)
Pressure sensors (5×)	Druck (Hoevelaken, The Netherlands)	Unik500 0–10 bar, A2	0.1% FS (0.01 bar)
Evaporator plates (16×)	Wakefield (Nashua, NH, USA)	120457	
Condensers (4×)	Boyd (Laconia, NH, USA)	M10-080SB	
Fan	HLU (Mücke-Atzenhein, Germany)	HF R 200-17 D Atex zone II	
Motorized control valve	END Armaturen (Bad Oeynhausen, Germany)	EBKG2D31X221025	
Accumulator 5 L	VARÉM (Limena, Italy)	R8005281S4000000	
Accumulator 1 L	VAREM (Limena, Italy)	V2001860S4000000	
Air separator	Spirotech (Helmond, The Netherlands)	Spirovent AAS125R	
Pressure regulator	Metalwork (Brescia, Italy)	Regtronic 1/4″	0.1 bar
Temperature sensor	Labfacility (West Sussex, UK)	thermocouples type T	±1 °C
Power supply evaporators	Eurotherm (Worthing, SD, USA)	Epack-1PH	±2% (0.4 kW)
Data acquisition system	National instruments (Austin, TX, USA)	cRio NI 9045	

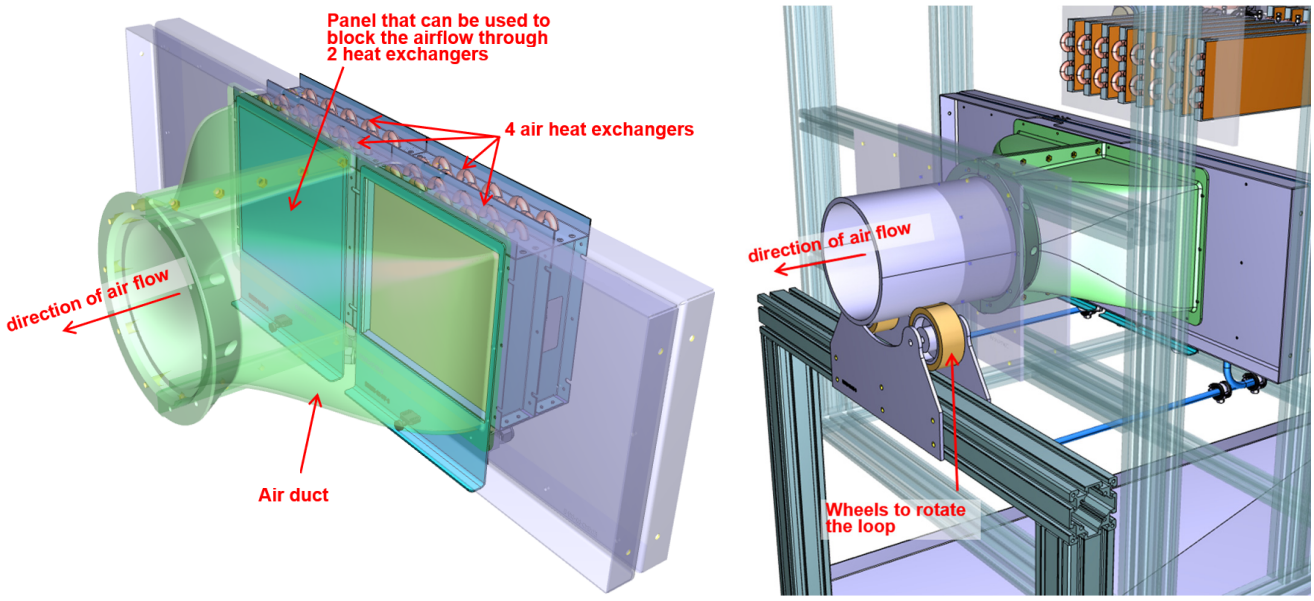

(**a**) (**b**)

Figure 5. (**a**) CADs drawing of the condenser section; (**b**) CAD drawing of the condenser section in the setup.

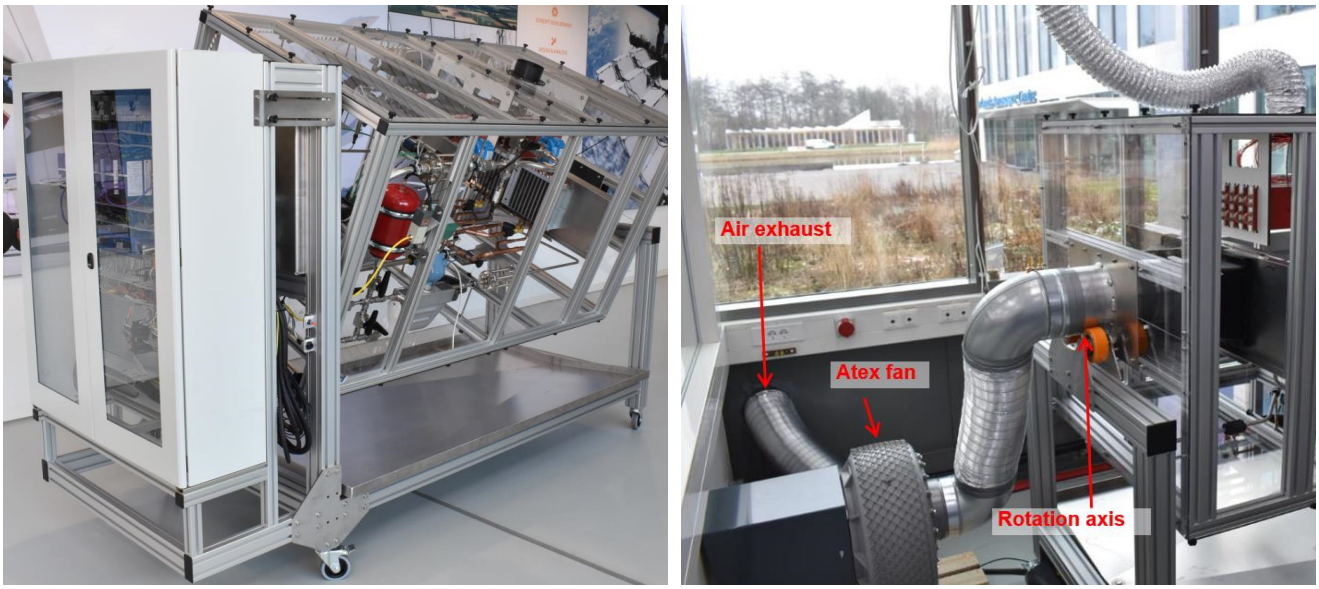

(**a**) (**b**)

Figure 6. (**a**) Photo of the 20 kW test setup in partially rotated (22.5°) orientation; (**b**) photo of the fan that is used to force air through the air heat exchangers.

3. Test Results with Accumulator

3.1. Instantaneous Full Power

The BRAVA cooling system must be able to handle variations in the heat load. The most extreme heat load variation is the instantaneous transition between full power on and off. Figure 7a shows the applied heater power to the evaporator. At t = 0.1 h, the heat load is increased from 0 to 20 kW, and at t = 1.1 h, it is reduced to 0 W. Figure 7b shows the control signals for the pump, the fan, and the bypass valve. The pump is set to 17%, which results in a mass flow of approximately 60 g/s (see Figure 8a). The fan is set to 70%, and the bypass valve remains closed during the test. Figure 8b shows

the measured temperatures at the two evaporator inlet branches (dashed and solid grey lines) and the temperatures at the outlets of the sixteen evaporator plates (solid-colored lines for eight evaporator outlets in branch 1, and dashed colored lines for eight outlets in branch 2). The black line indicates the saturation temperature, which is derived from the pressure at the evaporator outlet. At t = 0.1 h, the saturation temperature is set to 95 °C by controlling the pressure in the accumulator (which is increased from 1 bar to 3 bara—see Figure 9a). When the evaporator heater power is turned on, the evaporator outlet temperatures quickly rise until the saturation temperature is reached, and the liquid starts to boil. However, before the onset of boiling, the liquid is superheated to 115 °C, before it quickly drops to the saturation temperature of 95 °C. The same measurement was carried out multiple times, and very similar results were obtained each time, except that the amount of superheat varied (between 10 °C and 20 °C). This liquid superheat is further discussed in the next section.

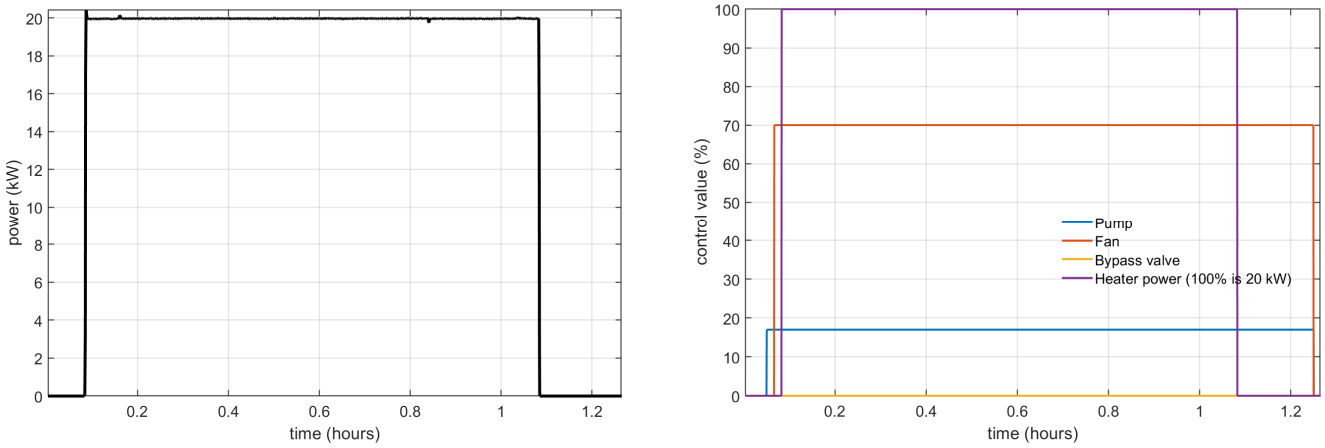

(**a**) (**b**)

Figure 7. (**a**) Applied evaporator heater power; (**b**) control signals.

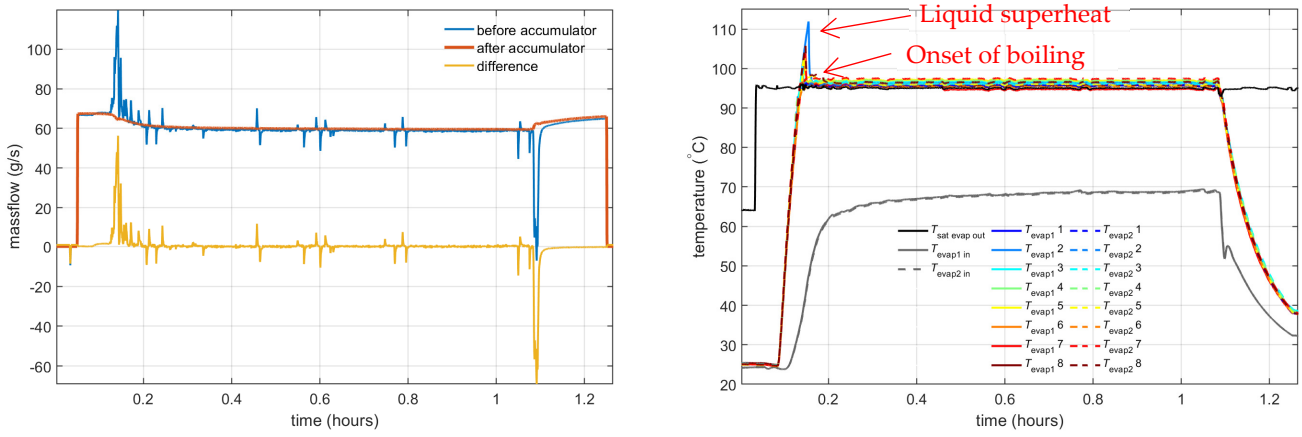

(**a**) (**b**)

Figure 8. (**a**) Measured mass flows; (**b**) measured temperatures.

Figure 10a shows the vapor mass fraction at the evaporator exit. This vapor mass fraction is calculated from the evaporator inlet temperature, the saturation temperature, the mass flow, and the evaporator heat input. The dashed lines indicate the bounds of the vapor mass fraction as a result of inaccuracies, assuming an uncertainty of the evaporator inlet temperature of ±1 °C, a pressure uncertainty of ±0.01 bar (this effect is negligible),

a heat input of ±0.4 kW, and a heat leak between 0 and 1.8 kW (this heat leak has been measured). Figure 10b shows the methanol liquid volume inside the accumulator. This volume is obtained by integrating the measured difference in the mass flows before and after the accumulator, and by dividing this mass by the liquid density. The dashed lines indicate the bounds of the accumulator volume as a result of inaccuracies, assuming an uncertainty in the measured flows of ±0.5 g/s. Because the measured difference between the mass flows is integrated over time, the accumulator volume uncertainty increases over time. In steady state, the offset between the two flowmeters is 0.79 g/s, and this offset is added to the mass flow difference.

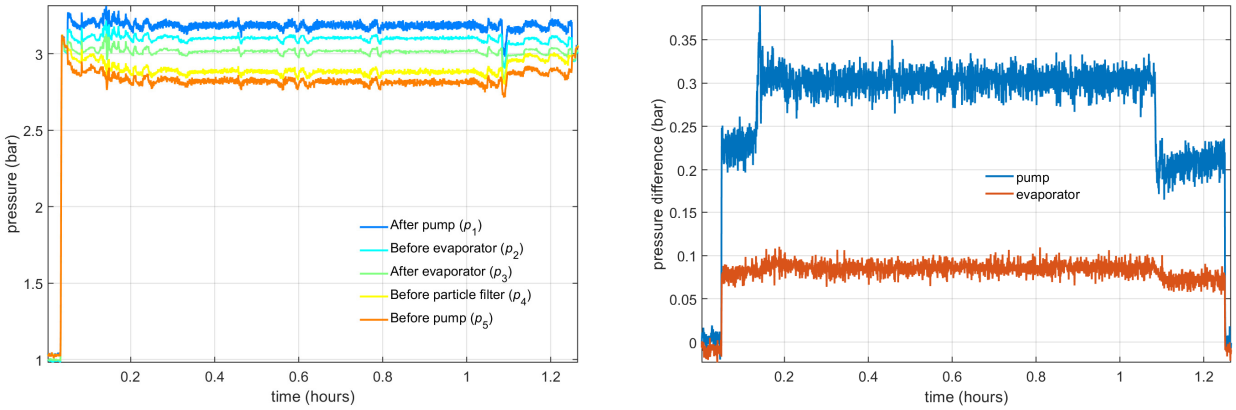

(**a**) (**b**)

Figure 9. (**a**) Measured pressures; (**b**) measured pressure difference over the pump and evaporator.

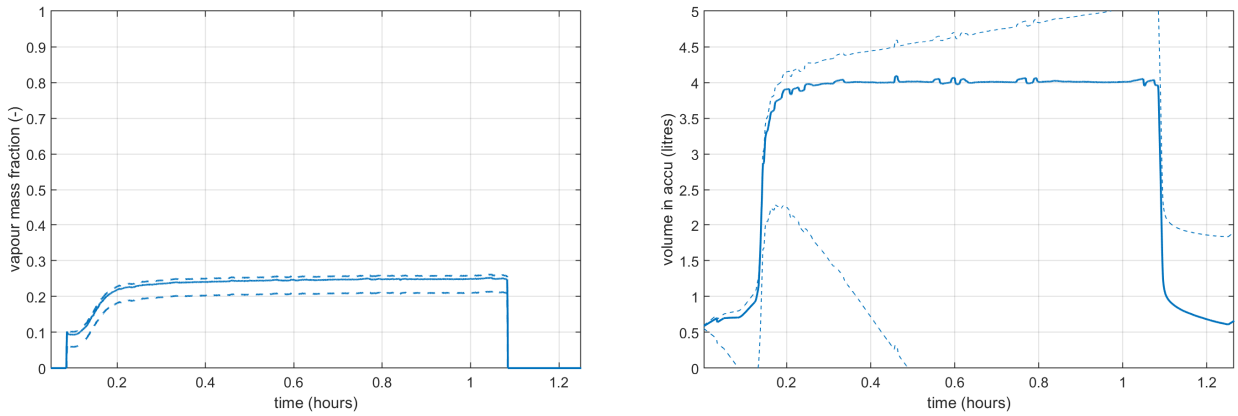

(**a**) (**b**)

Figure 10. (**a**) Calculated vapor mass fraction at the evaporator outlet; (**b**) methanol liquid volume in the accumulator.

3.2. Prevention of Liquid Superheat

In Figure 8b, liquid superheat is observed before the methanol starts to boil. This liquid superheat is caused by the lack of boiling nucleation sites on the smooth tubing wall of the evaporator. Furthermore, methanol is prone to liquid superheat, e.g., because of its relatively high surface tension. One of the methods to prevent liquid superheat is to inject small gas bubbles (e.g., N_2 or air) just before the evaporator. Figure 11 shows the measured temperature with the same test sequence as described in the previous section, except that a small amount (~16 mL) of N_2 gas is injected before the evaporator when

the liquid temperature reaches the boiling temperature. This gas injection prevents liquid superheat. The 20 kW system has an air separator that can expel the injected N_2.

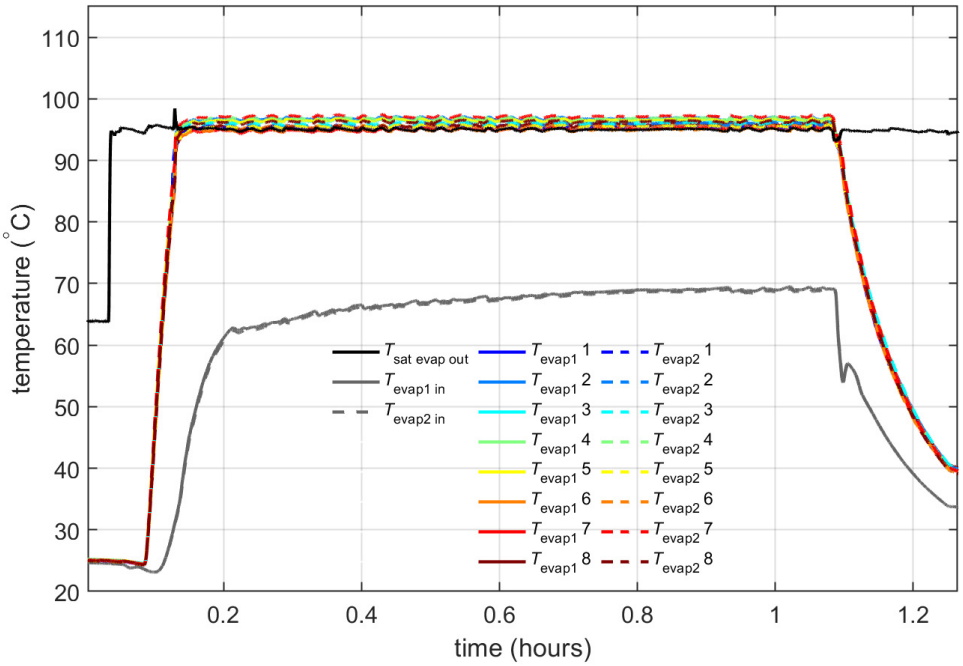

Figure 11. Measured temperatures.

Liquid superheat is very geometry-dependent, e.g., liquid superheat was not observed in tests with two-phase methanol with an evaporator made from bipolar plates from a fuel cell. A possible reason is that these bipolar plates have small, sharp-cornered gaps [5], which act as nucleation sites for boiling.

3.3. Controlling the Evaporator Inlet Temperature with the Bypass Valve or Fan Speed

In the measurements described in the previous sections, the liquid enters the evaporator with a temperature of around 70 °C. In the requirements for the 2-PC system [11], it is specified that the evaporator inlet temperature can be controlled between 75 and 85 °C. In the 20 kW setup, the evaporator inlet temperature can be controlled with two methods:

1. The fan speed can be varied; a lower fan speed results in less cooling capacity and thereby a higher evaporator inlet temperature. In an aircraft, this would be similar to reducing the airflow through the ram air heat exchanger with, e.g., a ram air door.
2. The condenser bypass valve can be opened. This increases the evaporator inlet temperature.

The fan and the bypass valve can be regulated via a PID controller that tries to control the evaporator inlet temperature to the setpoint value. Figure 12a shows the measured temperatures at the evaporator inlet and the outlet. Between t = 0.5 and 2 h, the evaporator inlet temperature is controlled by varying the fan speed, and the temperature is set to 75, 80, and 85 °C. Between 2.4 and 3.9 h, the inlet temperature is controlled by opening the bypass valve. Figure 12b shows the control signals to the fan and the bypass valve. This measurement shows that the evaporator inlet temperature can be controlled between 75 and 85 °C with these methods.

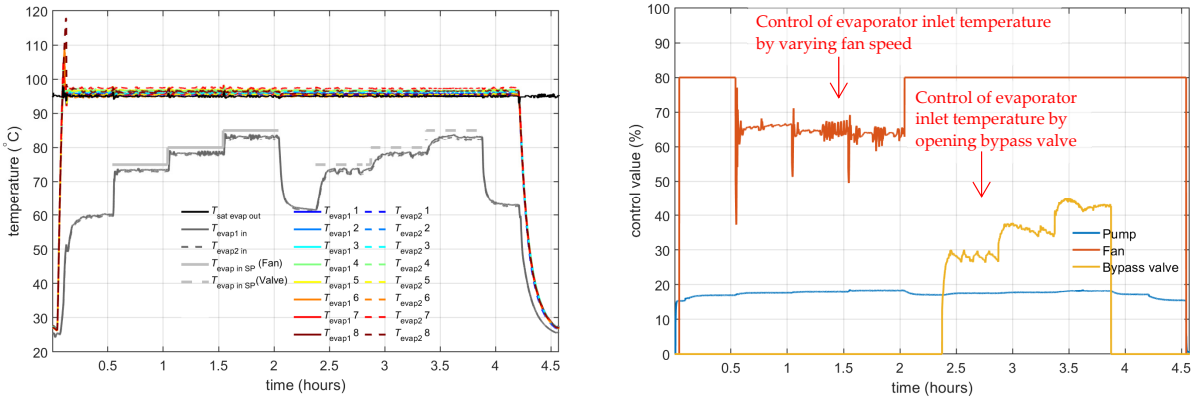

(**a**) (**b**)

Figure 12. (**a**) Measured temperatures; (**b**) control signals.

3.4. Influence of Orientation

In a two-phase cooling system, gravitational effects could influence the system, e.g., by causing dry-out of evaporators that are located higher than other evaporators. The 20 kW setup is designed so that it can operate in every orientation. For example, at the inlet of each evaporator is a flow restriction that consists of an orifice that has a diameter of 1.5 mm. The pressure drop due to this orifice can be calculated with [12]

$$\Delta p = \frac{8\,\dot{m}^2}{\rho_l\,\pi^2\,C^2}\left(\frac{1}{d^4_{\text{restriction}}} - \frac{1}{d^4_{\text{pipe}}}\right) \tag{1}$$

where $\dot{m}$ is the mass flow, ρ_l is the liquid density, $d_{\text{restriction}}$ is the diameter of the flow restriction, d_{pipe} is the diameter of the pipe, and C is the orifice discharge coefficient, which is approximately 0.6 for sharp-edged orifices. These flow restrictions result in a pressure difference of approximately 0.08 bar, which is larger than the pressure difference that can be caused in the evaporator by gravity (which is ~0.03 bar), and this ensures an equally distributed flow over all 16 evaporators in each orientation. Similar flow restrictions have also been successfully used in other systems [8,9].

Figures 13 and 14 show the measured temperatures with the same test sequence as in Section 3.1 'Instantaneous full power', except that the system is rotated with 90°, 180°, and 270° (see Figure 6 for a photo of a partly rotated system and the rotation axis). The results are very similar, which indicates that the system can operate in these orientations.

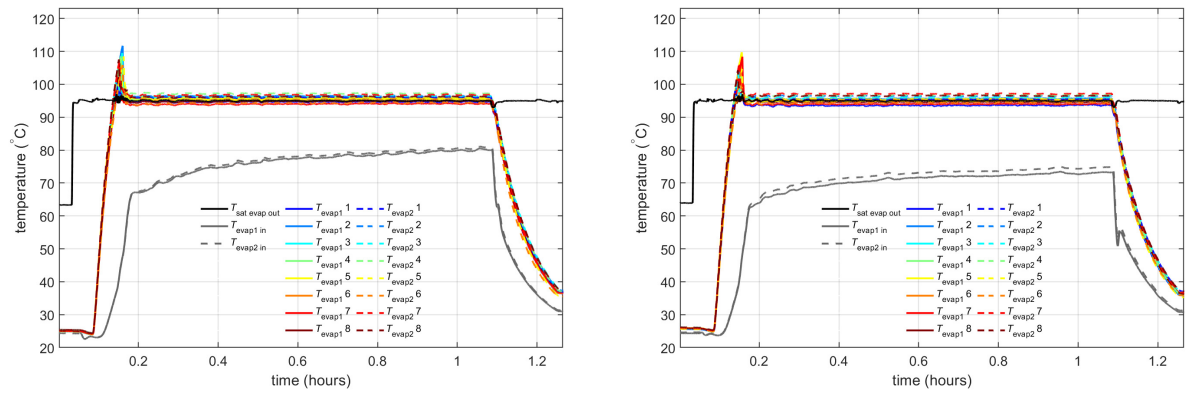

(**a**) (**b**)

Figure 13. Measured temperatures (**a**) with the system rotated 90°; (**b**) with the system rotated 180° ('upside down').

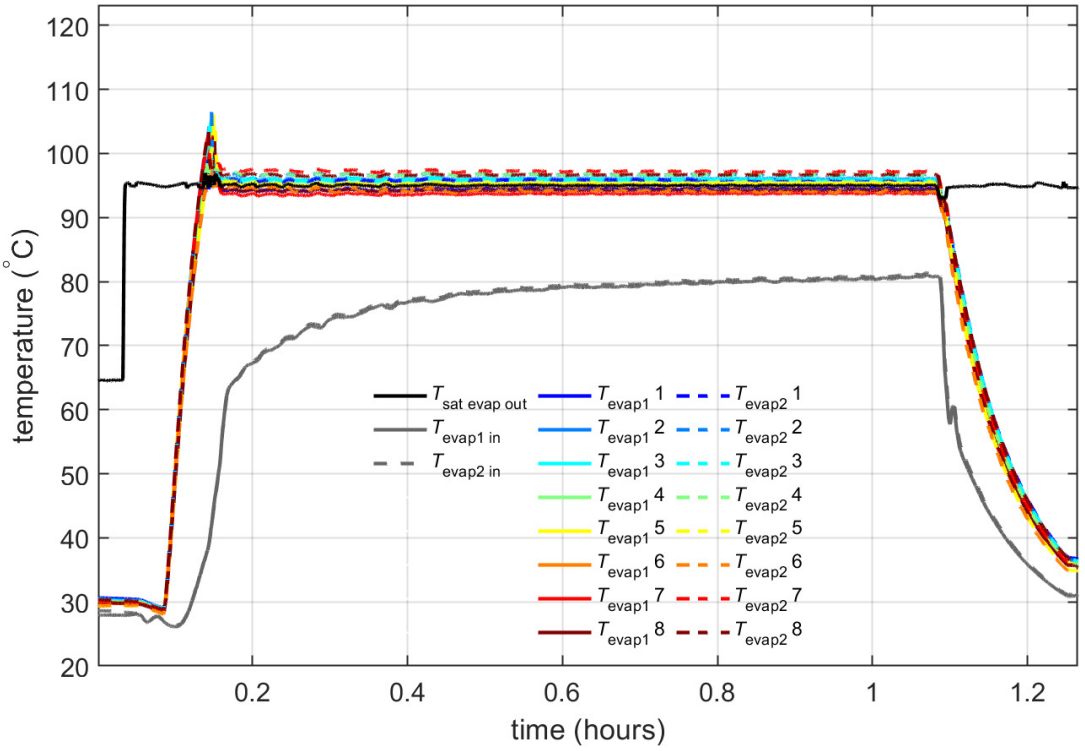

Figure 14. Measured temperatures with the system rotated 270°.

3.5. Influence of Blocked Condenser

A 2-PC system can have parallel condensers. The system should still function (albeit with a reduced heat rejection capacity) if the airflow through one of the condensers is blocked. The frictional pressure drop strongly increases with an increasing vapor mass fraction. When the airflow through a condenser is blocked, the vapor is not condensed back into liquid, and this results in a higher pressure drop than in the other condenser branches. Since there must be an equal pressure difference over each branch, this higher vapor fraction will result in a smaller mass flow through the blocked condenser (and a higher mass flow through the still-functioning condensers). As a result, the cooling system will remain functional even if the airflow through one of the condensers is blocked. In order to test this, a measurement similar to the test described in Section 3.1 ('Instantaneous full power') was carried out, except that the airflow through two of the four condensers is blocked by a metal plate (see Figure 5). Figure 15a shows the control values for the heater, pump, and fan. Because the airflow through half of the condensers is blocked, the maximum heat rejection capacity of the system is reduced to 16 kW (with 100% fan speed). Figure 15b shows the measured temperatures at the evaporators, and Figure 16 shows the measured temperatures near the condenser. The airflow through condenser 1 and 2 is blocked, and the temperatures at the outlets of these condensers ($T_{condOut1}$ and $T_{condOut2}$) are equal to the saturation temperature because the fluid is not cooled in these condensers. Additionally, the temperature where the flows from condensers 1 and 2 are combined ($T_{condOut12}$) is at saturation temperature. The temperatures at the outlets of condensers 3 and 4 ($T_{condOut3}$ and $T_{condOut4}$) are well below saturation temperature. The temperature of the combined flows from all four condensers ($T_{condOut}$) is around 80 °C. This measurement shows that the system still functions if the airflow through some parallel condenser branches is blocked.

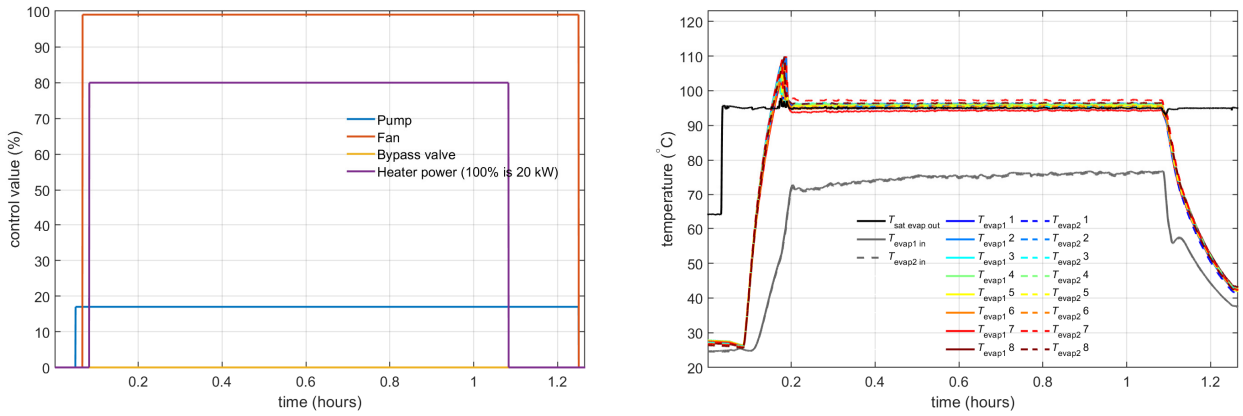

(**a**) (**b**)

Figure 15. (**a**) Control signals with blocked condenser; (**b**) measured evaporator temperatures with blocked condenser.

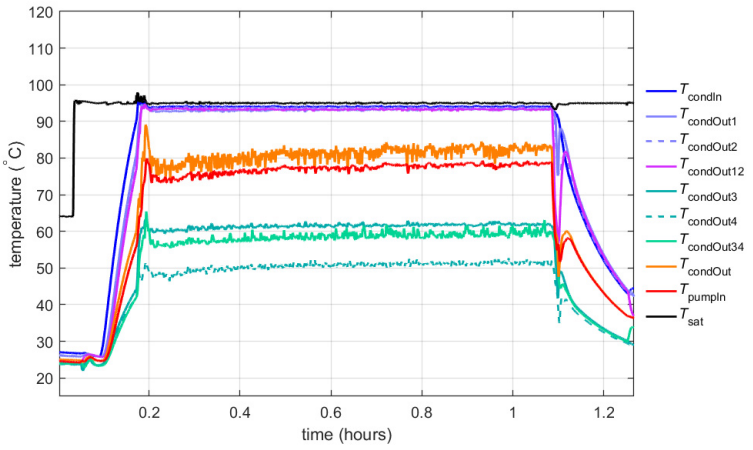

Figure 16. Measured condenser temperatures.

4. Test Results Without Accumulator

4.1. Background

In the previous sections, a configuration of the setup with an accumulator was tested. This accumulator controls the pressure (and thereby the saturation temperature) in the system and accommodates density changes (resulting from changes in liquid temperature and vapor fraction) of the fluid in the 2-PC system. The accumulator enables the loop to be completely filled with liquid (when no heat load is applied) and partly filled with vapor (when a heat load is applied). It is also possible to have a 2-PC system without an accumulator. Such a system results in a significant mass saving, not only because of the absent mass of the accumulator but also because of a large reduction in the fluid mass in the system (since a large part of the internal volume of the loop is filled with vapor) [5]. However, without an accumulator, the start-up and control of the saturation temperature/pressure in the system are not straightforward. A system with CO_2 as the coolant operating at a saturation temperature of around 20 °C has previously been successful tested by NLR [13] (to the authors' knowledge, there are no other descriptions of 2-PC systems without an accumulator available in the literature). In this system, the pressure in the system was controlled by the pump speed:

- If the pressure is higher than desired, the pump speed is increased. This reduces the vapor fraction in the system, which results in a lower pressure (and therefore a lower saturation temperature).

- If the pressure is lower than desired, the pump speed is decreased. This increases the vapor fraction, which results in a higher pressure.

When the liquid and vapor flows in a pipe have the same velocity (the homogeneous flow assumption), the vapor volume fraction ε can be analytically derived from the vapor mass fraction x:

$$\varepsilon = \frac{x\rho_l}{(1-x)\rho_v + x\rho_l} \tag{2}$$

where ρ_l is the liquid density and ρ_v is the vapor density. The homogeneous flow assumption is valid for plug/slug flow (which is usually encountered in microchannels) and bubbly flow. For annular flow, the vapor velocity is higher than the liquid velocity, and an estimation of the vapor volume fraction can be obtained by minimizing the kinetic energy of the flow, which results in the Zivi model [14]:

$$\varepsilon = \frac{1}{1 + \frac{1-x}{x}\left(\frac{\rho_v}{\rho_l}\right)^{2/3}} \tag{3}$$

Figure 17 shows the vapor volume fraction as a function of the vapor mass fraction according to the homogeneous and Zivi models. For methanol, the vapor volume fraction is almost constant (i.e., $\mathrm{d}\varepsilon/\mathrm{d}x$ is relatively small) for vapor mass fractions above 0.1. As a result, the pressure in the system cannot be controlled by varying the massflow (which results in varying the vapor mass fraction) when methanol is used as a coolant. For many applications, control of the saturation temperature is not required as long as a maximum temperature is not exceeded. However, for FC cooling, it is necessary to be able to control the saturation temperature. Besides varying the pump speed, there are other methods to control the temperature. These are discussed in the next sections.

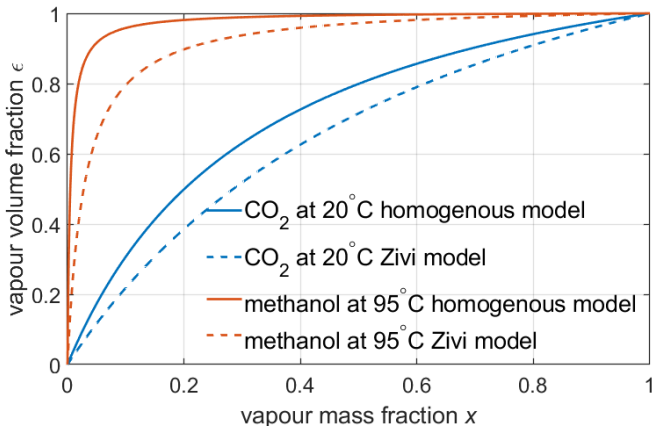

Figure 17. Vapor volume fraction as a function of the vapor mass fraction for methanol and CO_2 for homogeneous flow and according to the Zivi model.

4.2. Filling of the Loop

The test setup has a manual valve between the accumulator and the loop. During the tests without an accumulator, the valve is closed, and the accumulator is hydraulically separated from the rest of the system. This emulates a system without an accumulator. In order to obtain the required amount of fluid in the loop, the system is first operated with a heat load of 20 kW, with the valve between the loop and the accumulator open. The system contains 5 kg of methanol. Without a heat load, most of the methanol is inside the loop. When the heat load is applied, vapor is generated in the loop, which pushes liquid into the accumulator. When a steady state is reached, the valve between the accumulator and the loop is closed. The loop is now filled with vapor and liquid and contains approximately

1.5 kg of methanol, while the accumulator contains approximately 3.5 kg of methanol (this was determined by draining and weighing the methanol from the loop and the accumulator separately). Note that in an actual system without an accumulator, the required amount of fluid in the loop can be obtained by analysis, which requires an estimation of the internal volumes in the loop. When the loop is filled with approximately 1.5 kg of methanol and the manual valve between the accumulator and the loop is closed, the tests described in the next sections are carried out.

4.3. Instantaneous Full Power

Figure 18a shows the control signals for the pump, fan, bypass valve, and evaporator heaters. Figure 18b shows the measured temperatures, and Figure 19 shows the measured pressures. When the system is at rest, the pressure in the system is 0.25 bara. This is higher than the saturation pressure of 0.13 bara for pure methanol at 20 °C. The reason is that the system contains some air, e.g., because some air is dissolved in the methanol before it is introduced into the system. When the pressure in the system is below ambient pressure, this dissolved air is released from the methanol, which results in a pressure in the system above the saturation pressure from the methanol.

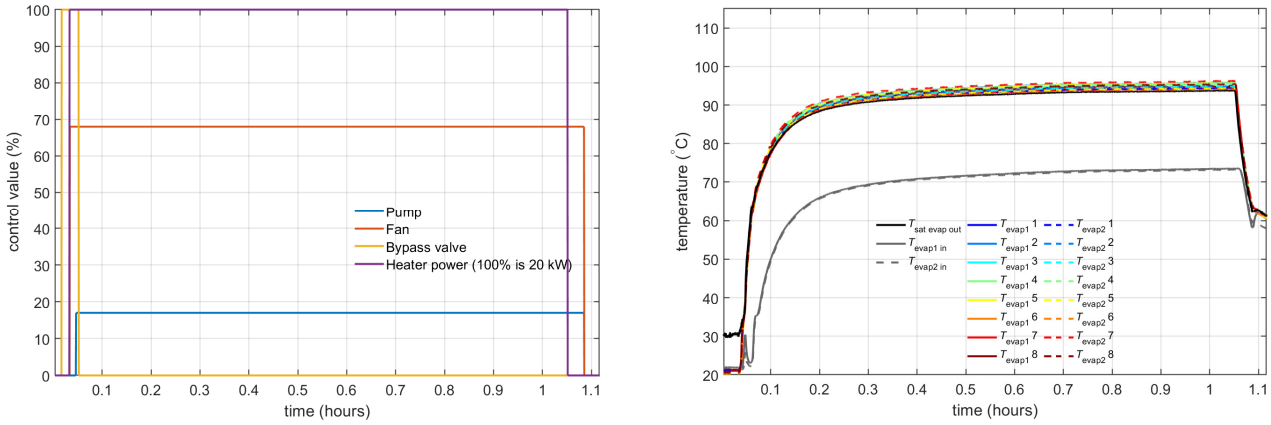

(**a**) (**b**)

Figure 18. (**a**) Control signals without accumulator; (**b**) measured evaporator temperatures without accumulator.

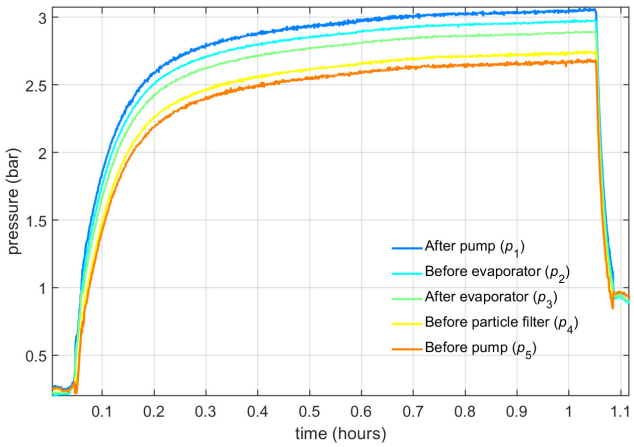

Figure 19. Measured pressures.

At t = 0.04 h, the heater power and fan are turned on. The heater power results in the evaporation of some liquid that was present in the evaporator, and the pressure and

saturation temperature in the system increases. After a minute, the pump is turned on. As a result, more liquid enters the evaporator, which partially evaporates and results in a quick rise in system pressure and saturation temperature. In contrast to a system with an accumulator, there is no liquid superheat. The saturation temperature continue rising until a steady-state temperature of around 95 °C is reached. Since there is no accumulator, the pressure and saturation temperature in the system cannot be directly set. Instead, they depends on the heat load and on fan speed. This is further discussed in the next section.

4.4. Control of Saturation Temperature with Fan Speed

In a system without an accumulator, the saturation temperature can be controlled by varying the airflow through the air heat exchanger. When the fan speed is increased, a larger fraction of the condenser will be filled with liquid, and this reduces the pressure in the system. A decrease in fan speed increases the pressure in the system. In an aircraft, this would be similar to reducing the airflow through the ram air heat exchanger with, e.g., a ram air door. Figure 20a shows the control signals during the test, and Figure 20b shows the measured temperatures. At t = 0.04 h, the heat load is set to 20 kW. Using a PID controller that regulates fan speed, the saturation temperature is controlled to the setpoint temperature of 90 °C. After 30 min, the setpoint for the saturation temperature is increased to 95 °C, and after another 30 min, the setpoint is changed to 85 °C. At t = 1.7 h, the heat load is decreased to 10 kW, and the setpoint for the saturation temperature is set to 90 °C, 95 °C, 85 °C, and 75 °C (each setpoint value is kept for 30 min). At t = 3.7 h, the heat load is decreased to 5 kW, and the setpoint for the saturation temperature is set to 75 °C and 65 °C. The measurements show that the saturation temperature can be controlled by the fan speed.

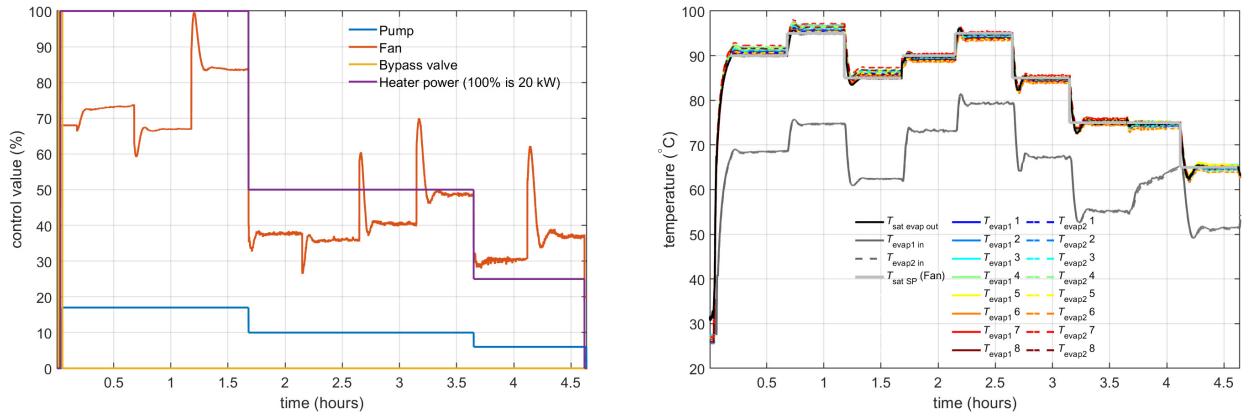

(**a**) (**b**)

Figure 20. (**a**) Control signals with saturation temperature control; (**b**) measured evaporator temperatures with saturation temperature control.

4.5. Control of the Evaporator Inlet Temperature

In a system without an accumulator, the saturation temperature can be controlled with the fan speed (see previous section). The evaporator inlet temperature can be controlled using two methods:

1. By varying the opening of the condenser bypass valve.
2. By varying the pump speed.

Figure 21a shows the measured temperatures during a test. At t = 0.04 h, the heat load is set to 20 kW. The fan speed is controlled so that the saturation temperature in the system is 95 °C. When the condenser bypass valve is closed, the evaporator inlet temperature is

approximately 75 °C. At t = 0.5 h, the setpoint for the evaporator inlet temperature is set to 80 °C, and at t = 1 h, the setpoint for the evaporator inlet temperature is increased to 85 °C. Figure 21a shows the measured temperatures during a similar test. In this test, the bypass valve remains closed. Instead, the mass flow is varied: At t = 0.55 h, the mass flow is reduced from 57 g/s to 40 g/s, and this reduces the evaporator inlet temperature to 66 °C. At t = 0.9 h, the mass flow is increased to 74 g/s, and this increases the evaporator inlet temperature to 78 °C. At t = 1.2 h, the mass flow is increased to 100 g/s, and this increases the evaporator inlet temperature to 81 °C.

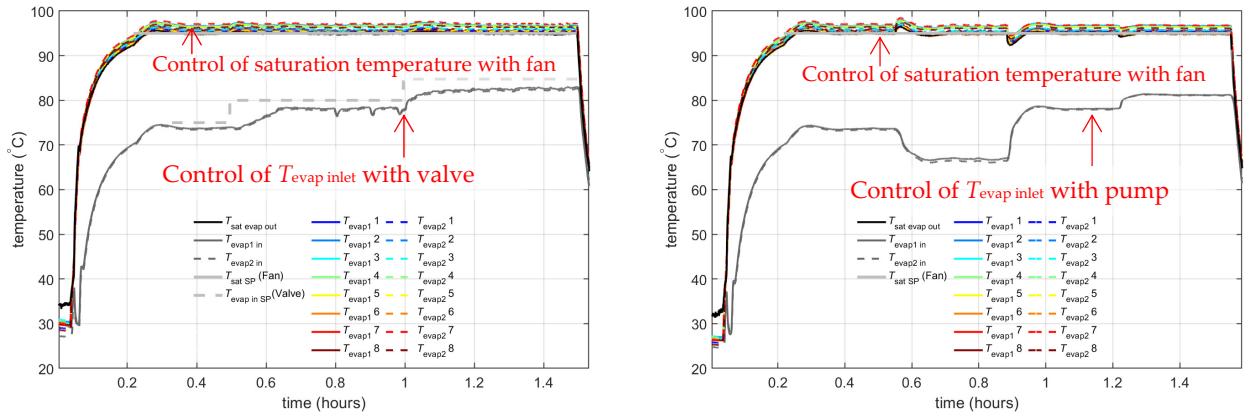

(**a**) (**b**)

Figure 21. Measured evaporator temperatures (**a**) with $T_{evap\ inlet}$ control using a valve; (**b**) with $T_{evap\ inlet}$ control using a pump.

4.6. Influence of Orientation

With an accumulator, the 2-PC system can start and operate in any orientation (see Section 3.4). Without an accumulator, the loop is partly filled with vapor, and the system can only be started when the pump is located at the bottom of the system, where gravity supplies liquid to the pump inlet. Once the pump has started and flow is generated, the 2-PC system functions in any orientation. This is illustrated by Figure 22, which shows the control signals and temperatures during a test where the system is rotated from 0° to 180° (i.e., to an 'upside down' orientation) at around t = 0.66 h.

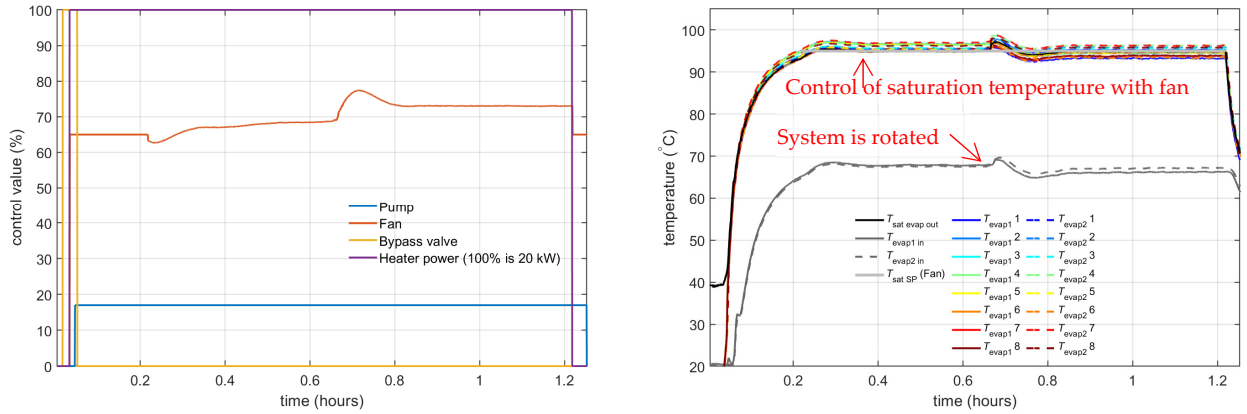

(**a**) (**b**)

Figure 22. (**a**) Control signals when rotating the system; (**b**) measured evaporator temperatures when rotating the system.

4.7. Imbalance in the Heat Load

In the previous tests, the evaporator heat load was applied to all 16 parallel evaporators. However, in an actual application, the heat load can be unevenly distributed over the different parallel branches, for example, due to a malfunction of a fuel cell. When there is no heat load in a parallel branch, it will cool down and become filled with liquid. In a 2-PC system without an accumulator, this liquid must come from other parts of the system, and this can result in dry-out. In order to test if the evaporator section can handle an imbalance in the heat load between the branches in a system without an accumulator, a 'worst case' test was carried out in which half of the evaporators received full power and the other evaporators suddenly received no power. Figure 23a shows the applied power levels during the test. First, the heaters for all evaporators in both branches were turned on. At t = 0.6 h, the heaters in branch 1 were turned off. After another 20 min, the heaters in branch 1 were turned on, and after another 20 min (at t = 1.2 h), the heaters in branch 2 were turned off. Figure 23b shows the measured temperatures. Even with this extreme imbalance in the heat load, none of the evaporator branches showed any sign of dry-out. This means that the system without an accumulator can handle an imbalance in the heat load.

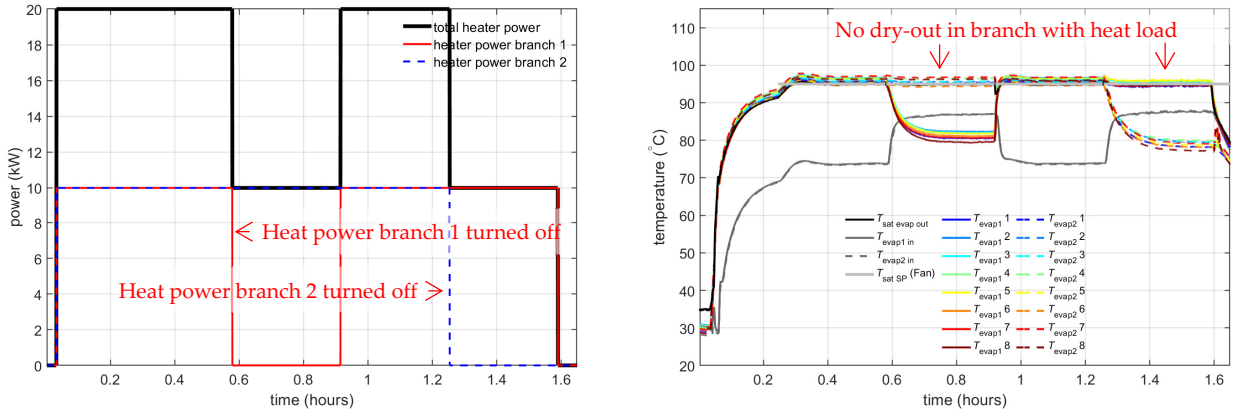

(**a**) (**b**)

Figure 23. (**a**) Evaporator heat input; (**b**) measured evaporator temperatures.

5. Test Results with Small Accumulator

In Section 3, test results with a 'normal-sized' accumulator were discussed. Such an accumulator enables the loop to be completely filled with liquid (when no heat load is applied) and to be partly filled with vapor (when a heat load is applied). The minimum volume of a 'normal' accumulator is equal to the volume of the system between the evaporator inlet and the condenser outlet (i.e., the part of the system where vapor can occur) plus the volume of the liquid needed for expansion due to temperature variations. For the 20 kW test setup, this minimum volume is approximately 3.5 L (see Figure 10b). In Section 4, test results for a system without an accumulator were discussed. Instead of using a 'normal-sized' or no accumulator, it is also possible to use a 'small' accumulator. Figure 24 shows the control signals and temperatures during a test with an accumulator with a volume of 1 L. This is smaller than the minimum required volume of 3.5 L to accommodate all fluid density changes. At the start of the test, the saturation temperature is set to 105 °C, which corresponds to a pressure of 4.1 bara (see Figure 25). The pressure in the loop is lower than the pressure in the small accumulator, and there is no liquid in the accumulator. When the heat load is applied (around t = 0.04 h), the pressure and thereby saturation temperature in the loop quickly start to rise until the pressure in the loop reaches the pressure in the accumulator. At that moment, some liquid will flow into

the accumulator and the saturation temperature in the loop can be controlled with the accumulator. The setpoint for the accumulator is then decreased in steps from 105 °C to 100, 95, and 90 °C. When the pressure in the accumulator is reduced, liquid flows into the accumulator. When the setpoint is set to 90 °C, the accumulator is completely filled with liquid, and the saturation temperature cannot be further reduced by the accumulator.

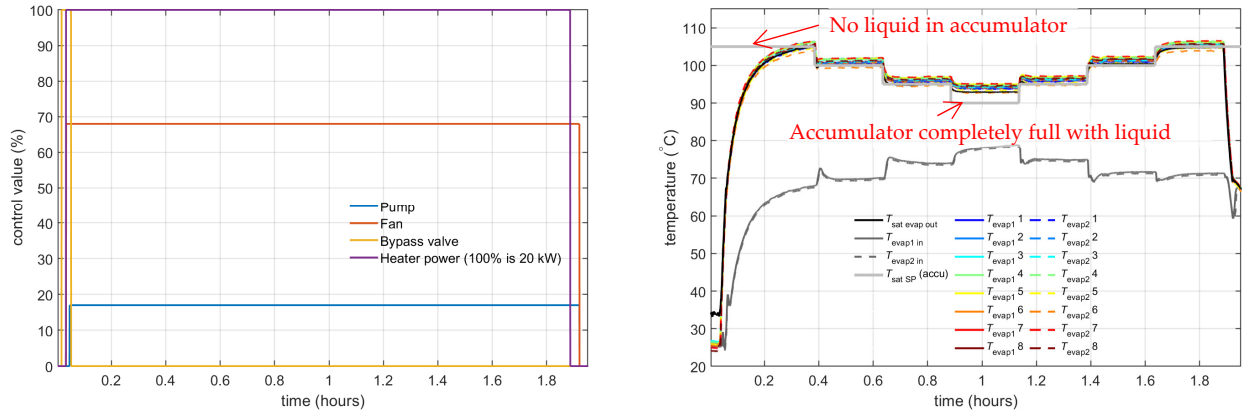

(**a**) (**b**)

Figure 24. Test with small accumulator (**a**) Control signals; (**b**) Measured evaporator temperatures.

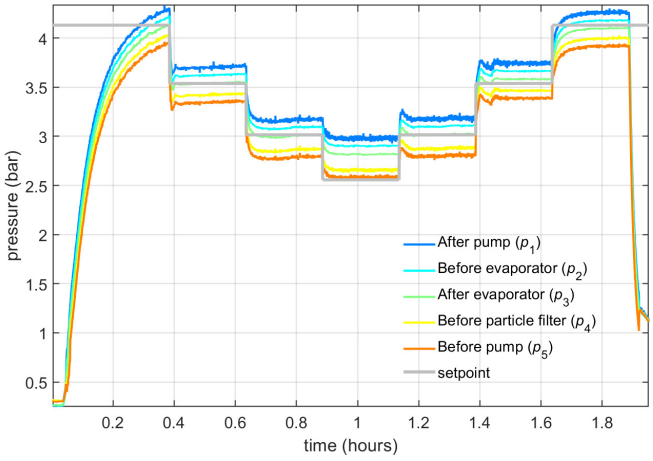

Figure 25. Pressures for the test with a small accumulator.

The advantage of a small accumulator compared to a normal accumulator is the reduction in mass; not only because of the smaller mass of the accumulator, but also because of a large reduction in the fluid mass in the system. Additionally, there is no liquid superheating in the system with a small accumulator. An advantage of a system with a small accumulator compared to a system without an accumulator is that it gives margin in the amount of fluid that is needed in the system, which can be convenient, e.g., in case of a small leak in the system. Furthermore, it gives an additional method to control the saturation temperature in the system.

6. Discussion

A comparison in a previous study [5] showed that the mass of a liquid EGW system is 35% higher than that of a 2-PC system with an accumulator and using methanol as a coolant. Furthermore, the mass of a liquid EGW system is even 2.4 times higher than the mass of a 2-PC system when the 'no accumulator' concept is used. In absolute numbers, the

2-PC system without accumulator has, according to the analyses, a 400 kg lower mass than a liquid EGW system for a FC-driven propulsion system with 2.4 MW electrical power [5]. An aircraft capable of carrying up to 100 passengers will have four of these propulsion systems [15], so the mass benefit could be more than 1600 kg per aircraft. Despite the much lower technical maturity, it is therefore considered worthwhile to further explore the 2-PC technology. In this paper, a 20 kW setup was used to investigate, e.g., temperature control, the influence of gravity, imbalance in the heat load (e.g., as a result of failure in some fuel cell stacks), and partly blocked airflow through the condenser. Additionally, several accumulator concepts were investigated, including the "no accumulator" and "small accumulator" concepts. In an aircraft, the ambient air (which can have a temperature between −55 °C and +50 °C) is forced through the fluid-air heat exchanger by the aircraft's forward motion or, when the aircraft is stationary, by a fan. The airflow through the heat exchanger can be regulated with ram air doors. In the 20 kW system, the variation in airflow is achieved by using a fan with controllable speed. With this controllable fan, the saturation temperature in the 20 kW system without an accumulator can be controlled. It is not yet clear if the controllable ram air doors can achieve the same temperature control as a controllable fan. However, it is expected that these doors have a sufficiently fast response time compared to the thermal response time of the fuel cells. The air that is forced through the condensers in the 20 kW system has a temperature of around 20 °C, which is very different from the −55 °C or +50 °C that can be encountered in an actual application. Unfortunately, it is difficult to conduct tests with these air temperatures, and it was considered out of scope for this project.

When a system without an accumulator is at rest, the pressure in the system is 0.25 bar, which is below the ambient pressure. If the system is not air-tight, air can leak into the system. Air leakage into the system has no influence on performance, since this air is expelled from the system via the air separator. However, an inleak of (moist) air into the system might have unexpected consequences, e.g., on corrosion. Another drawback of a system without an accumulator is that it can only be started when the pump is located at the bottom of the system and gravity supplies liquid to the pump inlet. However, once the pump has started and flow is generated, the 2-PC system functions in every orientation.

Besides the mass benefit, there are also some other benefits to using two-phase methanol. For example, when liquefied hydrogen (LH_2) is used as an energy source for the fuel cells, it has to be warmed from −250 °C to ambient temperature. This can be achieved with an electric heater, but it costs 8% of the electrical output of the fuel cell. Instead, the waste heat from a fuel cell could also be used to warm the cold hydrogen (only about 10% of the waste heat is required). Using liquid EGW to warm the LH_2 is extremely complex because the freezing point of EGW is relatively high, and the heat transfer coefficient of EGW becomes very low at low temperatures. As a result, a system with liquid EGW is prone to freezing issues. A system with two-phase methanol is much less prone to freezing issues because of its lower freezing point and higher heat transfer coefficient.

Using methanol as a coolant has several drawbacks. For example, it is flammable and toxic. Moreover, methanol has poor material compatibility with titanium and several aluminum alloys. This can be a significant issue since ram air heat exchangers are made from aluminum. For this reason, material compatibility tests (at 95 °C) with several aluminum alloys (and other materials that are used in a fuel cell cooling system) were carried out as part of the BRAVA project. Although no large issues with material compatibility have materialized so far, thorough compatibility tests must be conducted before this technology can be applied in aircraft.

The test results from the 20 kW system were used for the design of a two-phase methanol cooling system without an accumulator with a cooling capacity of 200 kW, which is currently under construction.

7. Conclusions

With a 2-PC system with a 20 kW cooling capacity, several concepts were tested. These tests show that saturation temperature control with a pressure-controlled accumulator works well and that the subcooling at the evaporator inlet can be controlled via the fan for the air heat exchanger or via the condenser bypass valve. Furthermore, the 20 kW system can operate in different orientations, and the system still functions if the airflow through some parallel condenser branches is blocked.

A system without an accumulator results in a huge mass saving, not only because of the absent mass of the accumulator but also because of a large reduction in the fluid mass in the system. Tests were carried out with a 20 kW system without an accumulator, and these tests showed that the saturation temperature can be controlled with the fan for the air heat exchanger.

Author Contributions: Conceptualization, G.M. and M.-B.B.; methodology, H.J.v.G. and S.S.; software, H.J.v.G. and T.L.; validation, H.J.v.G.; formal analysis, H.J.v.G.; investigation, H.J.v.G. and S.S.; resources, H.J.v.G.; data curation, H.J.v.G.; writing—original draft preparation, H.J.v.G.; writing—review and editing, T.L., G.M. and M.-B.B.; visualization, H.J.v.G. and T.L.; supervision, H.J.v.G.; project administration, H.J.v.G.; funding acquisition, H.J.v.G. All authors have read and agreed to the published version of the manuscript.

Funding: This BRAVA project is funded by the European Union's Horizon under grant agreement number 101101409. This publication reflects the authors' views. Neither the European Union nor the Clean Hydrogen Joint Undertaking can be held responsible for them.

Data Availability Statement: The raw data supporting the conclusions of this article will be made available by the authors upon request.

Conflicts of Interest: Author Georg Mühlthaler was employed by the company Airbus Commercial Aircraft and author Marcus-Benedict Buntz was employed by the company Aerostack GmbH. The remaining authors declare that the research was conducted in the absence of any commercial or financial relationships that could be construed as a potential conflict of interest.

References

1. Li, X.; Ye, T.; Meng, X.; He, D.; Li, L.; Song, K.; Jiang, J.; Sun, C. Advances in the Application of Sulfonated Poly(Ether Ether Ketone) (SPEEK) and Its Organic Composite Membranes for Proton Exchange Membrane Fuel Cells (PEMFCs). *Polymers* **2024**, *16*, 2840. [CrossRef] [PubMed]
2. Shang, Z.; Hossain, M.; Wycisk, R.; Pintauro, P.N. Poly(phenylene sulfonic acid)-expanded polytetrafluoroethylene composite membrane for low relative humidity operation in hydrogen fuel cells. *J. Power Sources* **2022**, *535*, 231375. [CrossRef]
3. Wang, Y.; Chen, K.S.; Mishler, J.; Cho, S.C.; Cordobes Adroher, X. A review of polymer electrolyte membrane fuel cells: Technology, applications, and needs on fundamental research. *Appl. Energy* **2011**, *88*, 4. [CrossRef]
4. Revolutionising Aviation: Propelling Towards Decarbonised Skies with H2-Fuelled FC. Available online: https://brava-project.eu/ (accessed on 7 January 2025).
5. van Gerner, H.J.; Luten, T.; Resende, W.; Mühlthaler, G.; Buntz, M.-B. System Analysis and Comparison Between a 2 MW Conventional Liquid Cooling System and a Novel Two-Phase Cooling System for Fuel Cell-Powered Aircraft. *Energies* **2025**, *18*, 849. [CrossRef]
6. van Es, J.; Pauw, A.; van Donk, G.; van Gerner, H.J.; Laudi, E.; He, Z.; Gargiulo, C.; Verlaat, B. AMS02 Tracker Thermal Con-trol Cooling System commissioning and operational results. In Proceedings of the 43rd International Conference on Envi-ronmental Systems, Vail, CO, USA, 14–18 July 2013.
7. Gorbenko, G.O.; Gakal, P.H.; Turna, R.Y.; Hodunov, A. Retrospective Review of a Two-Phase Mechanically Pumped Loop for Spacecraft Thermal Control Systems. *J. Mech. Eng.* **2021**, *24*, 27–37. [CrossRef]

8. van Gerner, H.J.; Kunst, R.; van den Berg, T.H.; van Es, J.; Tailliez, A.; Walker, A.; Ortega, C.; Centeno, M.; Roldan, N.; Cas-taneda, C.; et al. Development and Testing of a Two-Phase Mechanically Pumped Loop for Active Antennae. In Proceedings of the 52nd International Conference on Environmental Systems, Calgary, AB, Canada, 12–16 July 2023.
9. van Gerner, H.J.; de Smit, M.; van Es, J.; Migneau, M. Lightweight Two-Phase Pumped Cooling System with Aluminium Components produced with Additive Manufacturing. In Proceedings of the 49th International Conference on Environmental Systems, Boston, MA, USA, 7–11 July 2019.
10. van Gerner, H.J.; Cao, C.; Pedroso, D.A.; te Nijenhuis, A.K.; Castro, I.; Dsouza, H. Two-phase pumped cooling system for power electronics; analyses and experimental results. In Proceedings of the 30th International Workshop on Thermal Investigations of ICs and Systems (THERMINIC) 2024, Toulouse, France, 25–27 September 2024.
11. Resende, W. BRAVA deliverable report D2.1. In *PGS System Architecture and Requirements*; Airbus: Leiden, The Netherlands, 2023.
12. Munson, B.R.; Rothmayer, A.P.; Okiishi, T.H. *Fundamentals of Fluid Mechanics*, 7th ed.; Wiley: Hoboken, NJ, USA, 2020.
13. Donders, S.N.L.; Banine, V.Y.; Moors, J.H.J.; Verhagen, M.C.M.; Frijns, O.V.W.; van Donk, G.; van Gerner, H.J. Thermal Conditioning System for Thermal Conditioning a Part of a Lithographic Apparatus and a Thermal Conditioning Method. Patent US8610089, 2013. Available online: https://patents.google.com/patent/US8610089B2/en (accessed on 7 January 2025).
14. Zivi, S.M. Estimation of Steady-State Steam Void-Fraction by Means of the Principle of Minimum Entropy Production. *J. Heat Transfer.* **1964**, *86*, 247–251. [CrossRef]
15. Hydrogen Propulsion to Power Future Aircraft. Available online: https://www.airbus.com/en/innovation/energy-transition/hydrogen/zeroe/ (accessed on 12 January 2025).